PNAS RESEARCH ARTICLE | ECOLOGY

RNA sequencing analysis of viromes of *Aedes albopictus* and *Aedes vexans* collected from NEON sites

Sara H. Paull[a], Rachel R. Spurbeck[b], Nur A. Hasan[c], Kyle D. Brumfield[d], Lindsay A. Catlin[e], Michael J. Netherland Jr.[c], Anthony K. Smith[e], Katherine M. Thibault[a], and Rita R. Colwell[d,1]

Affiliations are included on p. 8.

Contributed by Rita R. Colwell; received March 25, 2024; accepted April 3, 2025; reviewed by Gregory D. Ebel and Gabriel L. Hamer

Climate change is significantly impacting the geographic range of many animal species and their associated microorganisms, hence influencing emergence of vector-borne diseases. Mosquito-borne viruses represent a potential major reservoir of human pathogens, highlighting the need for improved understanding of ecological factors associated with variation in the mosquito viral community (virome). Here, a subtractive hybridization method coupled with RNAseq of individual mosquito specimens was used to profile RNA viromes of individual co-occurring *Aedes albopictus* and *Aedes vexans* mosquitoes across a 2,000 km spatial scale. Samples were collected and archived by the National Ecological Observatory Network (NEON) from four ecologically variable sites in the Southeastern United States between 2018 and 2019. Results of multivariate analysis suggest that mosquito species are an important factor in RNA viral community composition. Significantly higher viral diversity was detected in *A. albopictus* compared to *A.vexans*. However, season, year, and site of sample collection did not show strong association with virome profiles, supporting the hypothesis that factors unique to the mosquito host species (e.g., larval habitat or vector competence) influence the structure of mosquito viromes.

Aedes albopictus | *Aedes vexans* | arbovirus | sequencing | mosquito

Significance

The risk of vector-borne viral infection is increasing globally as climate change and urbanization alter mosquito distribution and promote viral emergence. However, the diversity and ecology of mosquito-associated RNA viruses remain understudied. To this aim, we developed a subtractive hybridization method to enhance detection of rare viral sequences from total RNA sequencing of individual mosquitoes. This approach enables cost-effective, high-throughput virome analysis with reduced sequencing depth. Using data from the NEON network, we conducted a large-scale, interspecific comparison of mosquito viromes across diverse ecological contexts. Our findings advance understanding of mosquito viral ecology and support efforts to predict how climate-driven environmental changes may shape future patterns of viral emergence and disease transmission.

Mosquito-borne viruses are responsible for *ca.* 700,000 global deaths annually, and viruses such as yellow fever, dengue, West Nile, chikungunya, and Zika are emerging in many new geographical areas, driven in part by climate, urbanization, and globalization (1–5). Climate and population projection models have been used to estimate that 2.25 billion more people will be at risk of dengue in 2080, compared to 2015 (6). Genetic changes in viruses facilitating transmission to humans are an additional and less predictable driver of emergence and re-emergence of mosquito-borne viruses (4, 7). Detection and characterization of viruses, notably RNA viruses, are challenging, in part because microbial communities are traditionally defined employing culture-dependent methods. Development of nontargeted molecular tools to achieve virome characterization is necessary due to challenges associated with viral cultivation, and absence of globally conserved viral marker genes for targeted sequencing methods like 16S ribosomal RNA gene amplicon sequencing as is employed for bacteria. Cultivation-independent methods, e.g., metagenomics (DNA profiling) and metatranscriptomics (RNA profiling), have been developed, replacing isolation and culture with determining genomic composition (8, 9). The potential for emergence of mosquito-borne viruses underscores the importance of developing metagenomic and metatranscriptomic tools to investigate the genomics of mosquito-borne viruses and those environmental characteristics that influence their ecology (10). As climate change and urbanization drive the geographical distribution of mosquitoes and alter the ecosystem in which transmission occurs, it is important to establish a baseline profile of viruses in mosquito populations and identify factors influencing diversity of the viral communities. Importantly, a temporally and spatially persistent mosquito species-specific core virome will be essential to understand potential shifts in vector–virus–environment interactions, particularly for a notorious vector species such as *A. albopictus* (11).

Mosquito species relevant to public health and of interest for vector control agencies include the highly invasive *A. albopictus* and the floodwater nuisance mosquito, *Aedes vexans*. Both are members of the genus *Aedes* and known to feed extensively on humans (12, 13). *A. albopictus* is a documented vector of viral pathogens infectious to humans, including yellow fever, dengue, Zika, and chikungunya viruses (14, 15). While *A. vexans* is considered primarily a nuisance species, it is also a competent even if weak vector of West Nile, Zika, Rift Valley fever, and other viruses pathogenic for humans (16–18), as

Author contributions: S.H.P., R.R.S., N.A.H., K.D.B., K.M.T., and R.R.C. designed research; S.H.P., R.R.S., K.D.B., L.A.C., M.J.N., and A.K.S. performed research; S.H.P., R.R.S., N.A.H., K.D.B., L.A.C., M.J.N., A.K.S., K.M.T., and R.R.C. analyzed data; and S.H.P., R.R.S., N.A.H., K.D.B., L.A.C., M.J.N., A.K.S., K.M.T., and R.R.C. wrote the paper.

Reviewers: G.D.E., Colorado State University; and G.L.H., Texas A&M University.

The authors declare no competing interest.

[1]To whom correspondence may be addressed. Email: rcolwell@umd.edu.

This article contains supporting information online at https://www.pnas.org/lookup/suppl/doi:10.1073/pnas.2403591122/-/DCSupplemental.

Published May 12, 2025.

well as an important vector of dog heartworm (19). Climate warming has allowed many mosquito species, including *A. albopictus* and *A. vexans,* to expand their geographic ranges, with corresponding shifts in the viruses they carry (5, 6, 20). Concerningly, this is a trend expected to accelerate in coming years, with distributional changes generating new selective pressures on vector–virus relationships and increasing incidence of novel viruses carried by the vectors (3).

Studies of ecological factors influencing the viromes of these two mosquito species enable improved understanding of the structure of the mosquito virome and allow development of models to predict future shifts in the viromes and relevant public health response. Previous studies described the mosquito virome as containing both zoonotic and insect-specific viruses that are able to spill over into humans or indirectly modulate vector competence, impacting human disease risk (10, 21–23). Insect-specific viruses impact transmission of arboviruses by superinfection exclusion or insect immune system activation (22, 24). Superinfection exclusion, a mechanism of viral suppression, occurs when presence of one virus reduces or eliminates infection with a related virus, likely by competition for similar resources (10, 21, 25). Insect-specific virus distribution, host range, and impact on other viruses offer potential mechanisms for vector-borne disease control (26–28). Many open questions remain regarding the impact of insect-specific viruses on mosquito physiology and vector capacity, as well as potential evolution of a capacity to infect vectors (10). Clearly, mosquito virome ecology is an important component of a One Health approach to arboviral control (21).

The objective of the study reported here was to identify ecological determinants of the viral community of two mosquito species of public health significance, namely *A. albopictus* and *A. vexans*. Virome profiles of archived mosquito samples collected by the US NSF National Ecological Observatory Network (NEON) between 2018 and 2019 at four sites in the southeastern United States were characterized using nontargeted RNAseq methods to evaluate incidence of RNA viruses associated with mosquitoes. The analyses represent a combination of in-depth sequencing over a large spatial extent by analyzing metatranscriptomes of individual mosquitoes after host RNA depletion, thus expanding the capacity to understand spatial scale and ecological drivers of core viromes of these mosquito species.

Materials and Methods

Site Description and Sample Collection. Samples were collected by the NEON program following the Mosquito Sampling Protocol (29). NEON, a national observatory, provides a diversity of open access, continental-scale, ecological data and samples collected using standardized methods across 47 terrestrial and 34 aquatic sites. The samples used in the study reported here were collected at five terrestrial sites where the two focal vector species co-occur. Mosquitoes were collected every two to four weeks using Centers for Disease Control and Prevention light traps (John Hock, Gainesville, FL) baited with dry ice and set at dusk, followed by sample collection and trap resetting at dawn the next day. Samples were transported on dry ice to the laboratory facility and stored at −80 °C. All mosquito species were taxonomically identified using chill tables and subsequently pooled by site, collection event, species, and sex for ultimate accession by the NEON Biorepository, Arizona State University (30).

A. vexans and *A. albopictus* samples included in this study were collected between 2018 and 2019 in both early (March through early August) and late (late August through early December) seasons from five NEON sites, including the Smithsonian Environmental Research Center (SERC; latitude, longitude: 38.89013, −76.56001) and the Smithsonian Conservation Biology Institute (SCBI; latitude, longitude: 38.89292, −78.13949) in Maryland, Talladega National Forest (TALL; latitude, longitude: 32.95047, −87.39326) in Alabama, Lyndon B. Johnson National Grassland (CLBJ; latitude, longitude: 33.40123, −97.57) in Texas and Oak Ridge National Laboratory (ORNL; latitude, longitude: 35.96413, −84.28259) in Tennessee (Fig. 1 and *SI Appendix*, Table S1). Three replicate individuals were included for each species by season, year, and site combination for a total of 95 individuals (a single *A. albopictus* individual from CLBJ was lost during handling). In 2018, insufficient *A. vexans* mosquitoes were collected from SERC and therefore samples from SCBI, the NEON site nearest to SERC, were included. To avoid confounding the virome data generated from the SCBI samples (SCBI_2018_29_AEDVEX_F_A_01, SCBI_2018_41_AEDVEX_F_A_01, SCBI_2018_44_AEDVEX_F_A_01), these samples were removed from the geographical analysis. Whenever possible, a single individual was selected per vial containing no more than 20 mosquitoes to reduce cross-contamination among collectively stored samples (mean ± SD = 3.3 ± 3.1 individuals per vial) and, in some cases, two to three replicates from one vial.

Sample Processing, RNA Preparation, and RNA Sequencing. Individual mosquitoes (*A. vexans*, n = 48; *A. albopictus,* n = 47) were homogenized in 2 mL tubes with a steel bashing bead and 200μL DNA/RNA Shield (Zymo Research Corp, CA) using a 5 mm stainless steel bead and TissueLyser II (Qiagen, Germany) at the following intervals: 2 × 5 min at 25 Hz, rest on ice 1 min in between). Homogenates were allowed to stand for 5 min at room temperature (25 °C) before centrifugation at 3,000×*g* for 5 min at 4 °C. The supernatant was transferred to a new Rnase/Dnase free 1.5 mL centrifuge tube and centrifuged at 16,000×*g* for 2 min at 4 °C. The supernatant was transferred to an Rnase/Dnase free 96-well plate, a separate well for each sample. Lysates were split into two aliquots. From one aliquot, RNA was extracted using the QIAamp Viral RNA Mini Kit (Qiagen, Germany), according to the manufacturer's instructions, without carrier RNA. For quality assurance, a nuclease-free water control was included with each extraction batch.

RNA samples were mosquito host RNA- and high abundance microbial RNA-depleted prior to library preparation, employing subtractive hybridization (31). Briefly, genomic DNA was extracted from each mosquito species and purified using the QIAamp DNA extraction kit with RNase A treatment (Qiagen, Germany). Purified unfragmented mosquito DNA extracts were added to the respective total RNA preparations such that DNA and RNA had equivalent concentrations. The DNA:RNA mixtures were heat-denatured at 95 °C for 2 min and hybridized at 65 °C for 10 min. The RNA:DNA hybridized samples were allowed to cool at 37 °C. RNase H was added and allowed to stand for 5 min at 37 °C after which the RNase H was heat inactivated at 65 °C for 10 min. The remaining DNA was depleted by adding DNase I at 37 °C for 30 min. RNA was cleaned and concentrated using the Nucleospin PCR cleanup kit (Macherey-Nagel, Germany). RNA was quantified using a Qubit RNA High Sensitivity Assay Kit (Thermo Fisher Scientific, MA).

As control for the method and to ensure the subtractive hybridization removed vector RNA but retained viral RNA, two additional samples of *A. vexans* RNA were spiked with a synthetic version of the complete SARS-CoV-2 RNA genome (Exact Diagnostics) and treated by subtractive hybridization to remove *A. vexans* RNA and recover virus RNA. The samples were tested by qPCR specific to SARS-CoV-2 to quantify virus before and after subtractive hybridization.

RNA-sequencing libraries were prepared for the 95 mosquito RNA samples using the KAPA RNA HyperPrep Kit (Roche, IN), following the manufacturer's instructions. The libraries were quantified and size distribution confirmed by a high-sensitivity DNA bioanalyzer assay (Agilent, CA). The libraries were sequenced by EzBiome Inc. (Gaithersburg, MD) on a NovaSeq 6000 sequencer (Illumina, CA) and employing 150 base paired-end reads, targeting sequencing depth of at least 50 million clusters of paired-end reads per sample reads.

Sequence Processing and Viral Contig Identification. Metatranscriptomic taxonomic profiling was done using the EzBioCloud database, as previously described (32). Briefly, the profiling process was initiated by surveying the potential presence of bacterial and archaeal species for each raw metagenomic sample read using Kraken2 (33) and a prebuilt core gene database (34) containing k-mers (k = 35) of reference genomes obtained from the EzBioCloud database (35). Fungal and viral complete genomes from the NCBI Reference Sequence (RefSeq) collection (https://www.ncbi.nlm.nih.gov/refseq/) were added to the Kraken2 database.

Any organism with at least 1 k-mer of size 35 classified in any of the samples was considered a potential candidate. A custom Bowtie 2 database (36) was constructed using core genes and genomes from those organisms detected during the initial survey step. All samples were mapped against the Bowtie 2 database

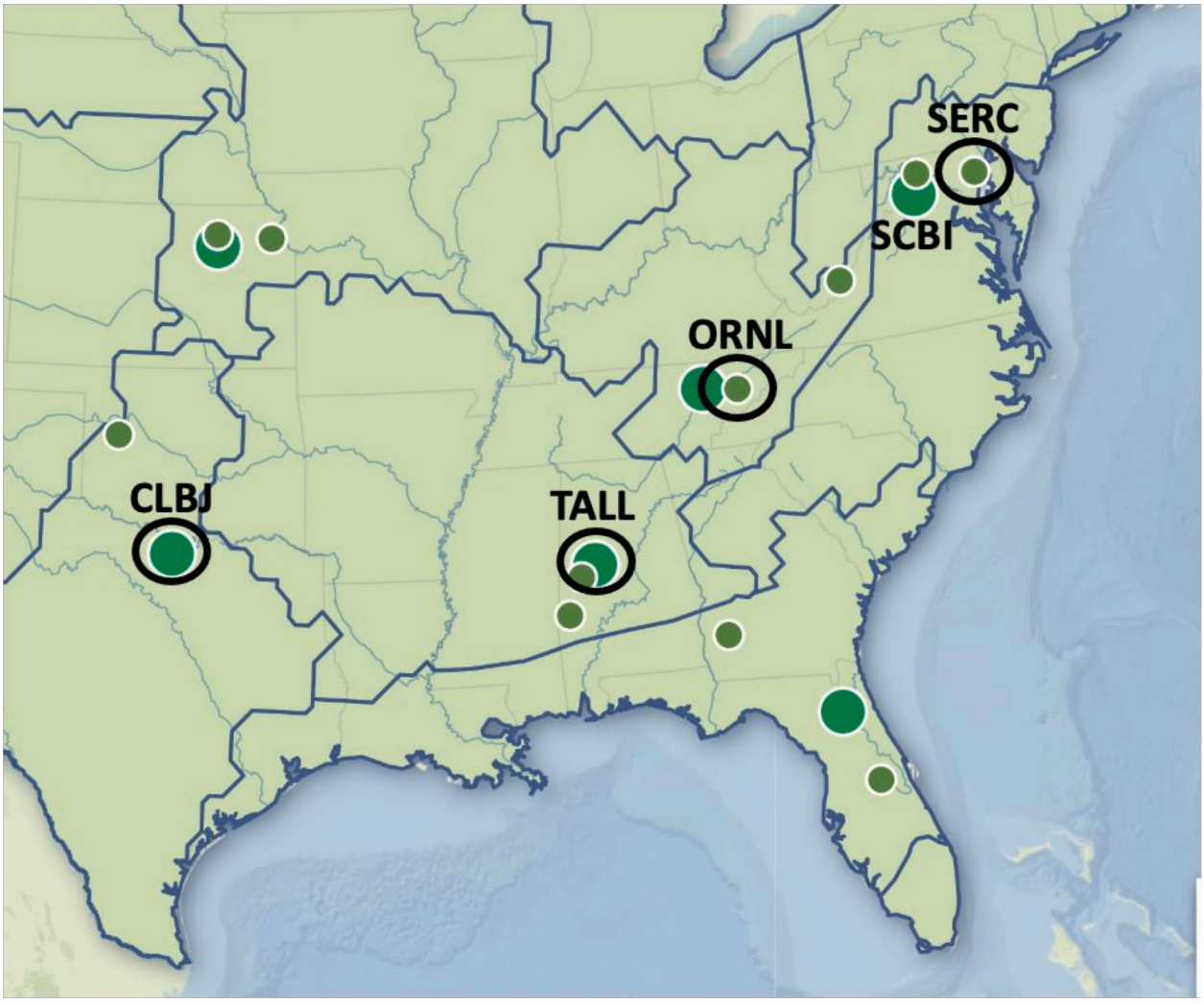

Fig. 1. Map of study area showing the four NEON sites from which mosquitoes were collected during 2018–2019. Larger circles indicate "core" sites sampled every two weeks during the active mosquito season, while smaller circles indicate "gradient" sites sampled every four weeks. Due to lack of sufficient samples of *Aedes vexans* collected at SERC in 2018, a total of three individuals were sequenced from the nearby SCBI site. NEON is a national observatory with ecological sampling occurring at 47 terrestrial and 34 aquatic sites spread across 20 ecoclimatic domains. Blue lines delineate the ecodomain boundaries, and sites without circles are areas where mosquitoes are collected by NEON but with fewer replicate samples for both species to include in this project.

using the "–very–sensitive" option and quality threshold of phred33. Sequence Alignment/Maptools v1.9 [SAMtools (37)] was used to convert and sort the output BAM (Binary Alignment and Map) file. Coverage of mapped reads against the BAM file was achieved using Bedtools (38). Organisms were considered present at the species level if mapped sequencing reads covered at least 1% of their reference genomes. For mapped sequencing reads covering less than 1% of the reference genome, down to a single read, the organisms were classified at the genus level and labeled as unclassified species under their respective genera. Abundance proportions were normalized using the reference length. For viral and fungal references, genome size was used, and for bacteria and archaea, the sum of the length of all core genes was used.

Metagenome-Assembled Genome (MAG) Taxonomic Profiling with Lazypipe. Given the relative lack of viral representation in many sequencing databases, two approaches were used to characterize the virome. First, the Lazypipe method, described in ref. 39 and designed to capture known and novel viruses, was used. Reads were preprocessed and trimmed using fastp v0.21.1 (40) and assembled into contigs using MEGAHIT v1.2.9 (41) with default options. Coverage of contigs was calculated by aligning trimmed reads with Burrows-Wheeler Aligner Minimum Exact Match v0.7.17-r1188 [BWA-MEM (42)] and calculating read coverage with SAMtools v1.9 (37). Contigs with less than 90% read coverage and mapping quality score of less than 30 were discarded.

Contigs were classified using Centrifuge v1.0.3-beta with the nucleotide (nt) centrifuge database (43). Secondary classification using Blastn with nt database (44) was run for those contigs without Centrifuge hits and Centrifuge and Blast results were combined to assign species to a contig.

Trimmed reads were aligned to MEGAHIT contigs with BWA-MEM, excluding alignment scores less than 40. Secondary and supplementary alignments were filtered with SAMtools to eliminate erroneous alignments. SAMtools idxstats was used to obtain the number of reads aligned to each contig. Centrifuge and Basic Local Alignment Search Tool (BLAST) identification results were used to associate read counts with taxa. For each sample alignment results, reads from contigs with the same taxon were merged, and a final read count matrix was produced by combining the results.

Taxonomic Profiling with RVDB. In the second approach, the Reference Viral Database (RVDB) was used to characterize the virome and establish taxonomy. For quality assurance, reference genomes present in RVDB were aligned against the National Center for Biotechnology Information (NCBI) Nucleotide Collection database (nr/nt) (version 5 accessed 31 January 2022) using the "blastn" function from the Basic Local Alignment Search Tool (BLAST+ v.2.15.0). Based on these BLAST search results, after reviewing the top hits, 26 reference sequences from the RVDB were identified as nonviral and subsequently removed from the local RVDB for further analysis. Reads trimmed with fastp were aligned to species references from RVDB v22.0 (45) using Bowtie2 v2.4.4 aligner with default options (36). Improperly paired reads and bases with a quality score below 13 were filtered out of the alignments using SAMtools (37). A Q score of 13 or higher corresponds to an error rate of 5% or less. This threshold was chosen because it aligns with the

conventional alpha value of 0.05 used in statistical analyses, which indicates a 5% probability of a Type I error (false positive). Coverage and depth metrics were calculated using SAMtools coverage to obtain the number of reads aligned and percent of genome coverage for each reference. The total number of references with correct BLAST hits was compared to the total number of references in the RVDB database. For a species to be verified in its sample alignment, a minimum of 10% of all references for that species in the RVDB database needed to yield >50 reads aligned and >20% coverage for at least one of the samples used for alignment. Prior to applying the filtering criteria, the results suggested the presence of several viruses (e.g., oropouche virus) deemed improbable based on their ecology and the lack of detection in the NEON mosquito pathogen status data product (46). The analyses focused on RVDB results where the strictest criteria were employed to determine the presence of viral species.

Data Analysis. A rarefied species richness for each sample was calculated using the "vegan" package rarefy function in R (47, 48). The richness values were compared by species, season, and year using the Wilcoxon test and across sites using the Kruskal–Wallis test. Nonmetric multidimensional scaling (NMDS) with Bray–Curtis dissimilarity matrix was employed to visually assess patterns in viral occurrence across variables, using the "vegan" package metaMDS function. Differences between groups were assessed using principal coordinate analysis (PcoA) and permutational multivariate ANOVA (PERMANOVA) employing capscale and adonis2 functions along with analysis of dispersion using the permutest function of the "vegan" package. All analyses were performed using R v4.3.0.

Results

Subtractive Hybridization RNA Sequencing Enriches Viral Read Outputs. For controls, two *A. vexans* samples containing RNA concentrations of 42.1 and 4.8 ng/μL were spiked with approximately 2000 copies of SARS-CoV-2 RNA. After subtractive hybridization treatment, mosquito RNA content of both samples was below detection when tested using Qubit RNA High Sensitivity Kit, confirming exogenous RNA removal. However, after subtractive hybridization treatment, SARS-CoV-2 RNA was detectable by qPCR in both samples at similar levels (2545.5 ± 177.4 and 3850.1 ± 641.9 viral copies present in the total sample), confirming that viral RNA remained in the samples.

The average RNA concentration from 95 individual mosquitoes was 16.0 ± 11.6 ng/μL for *A. vexans* and 13.3 ± 7.8 ng/μL for *A. albopictus*. After subtractive hybridization, RNA concentrations of all samples were below 250 pg/μL, sufficient for creating RNAseq libraries. A total of 10,950,862,866 sequencing reads were generated, with an average of 115,272,241 reads per sample and an average sequence length of 151 base pairs (bp). After trimming, average reads per sample were 57,084,871 with average sequence length of 103 bp. Metagenome assembly yielded an average number of contigs of 35,581 per sample. Sequencing results showed either a few or no contigs aligned to either *A. vexans* (median 0%, mean 0.02%) or *A. albopictus* (median 0.11%, mean 0.15%), indicating successful host RNA removal. The distribution of mapped reads by domain demonstrated most were viral (92.4 ± 12.9%), with fewer bacterial (7.6 ± 12.9%), fungal (0.3 ± 0.3%), or archaeal (0.001 ± 0.001%) reads. Residual bacterial reads likely represent a discrepancy between the reference DNA microbiome and the individual mosquito microbial RNA.

Virome Community Diversity and Composition Relative to Mosquito Hosts. Using the available generalized workflow for the Lazypipe method described in ref. 39, no novel viruses were detected in this set of mosquito samples (*SI Appendix*, Fig. S1). Additional validation steps of the Lazypipe dataset were performed, involving secondary classification of contigs and read alignments to targeted reference genomes. For most identified taxa, the validation supported their presence. However, for dengue virus, these additional steps revealed that the original matches were based on fractional (<1%) coverage (159 bp of a 10,766 bp sequence), and subsequent BLAST searches against the NCBI nr database indicated that the only dengue sequence alignment with significant coverage (93 bp of a 219 bp partial sequence) had poor depth. Consequently, we deemed the evidence insufficient to support definitive detection of dengue virus in the dataset.

Twenty viruses were detected in the 95 samples analyzed using the RVDB dataset. The viruses found to be present in both mosquito species were Mourilyan virus and pittosporum cryptic virus–1 (Figs. 2–4). Viruses detected in all *A. albopictus* samples were *A. albopictus* anphevirus, Aedes flavivirus, guato virus, and Wenzhou sobemo-like virus 4 (Figs. 2–4). A majority of *A. albopictus* hosted Kaiowa virus, nea chili luteo-like virus, Mourilyan virus, and Guangzhou sobemo-like virus (Figs. 2–4). In contrast, fewer viruses were detected in *A. vexans* and none in most samples tested (Figs. 2–4). *A. vexans* samples collected from the SCBI site were outliers because of the lack of *A. albopictus* sequenced from the site and were excluded from further analysis.

The rarefied species richness values from the RVDB dataset showed no difference according to location (χ^2 = 0.48, df = 3, P = 0.92), season (W = 1,030, P = 0.83), or year (W = 1,049, P = 0.96, *SI Appendix*, Fig. S2). Richness was significantly higher for the invasive vector, *A. albopictus* (Rarefied richness ± S.D. = 4.12 ± 0.88), relative to *A. vexans* (Rarefied richness ± S.D. = 0.50 ± 0.88; W = 2,011, P < 0.001). Similar results were obtained using Lazypipe dataset (*SI Appendix*, Figs. S3–S5) (site: χ^2 = 3.26, df = 3, P = 0.35; season: W = 1,117, P = 0.64; year: W = 947, P = 0.40; vector species: W = 1,880, P < 0.01).

Ordination of the data was used to visualize the structure of the mosquito virome by mosquito species, space, and time (Fig. 5). Viral communities grouped by species (Fig. 5 and *SI Appendix*, Fig. S6), and, in either dataset, both species (RVDB: $F_{1,51}$ = 3.40, P = 0.001; Lazypipe: $F_{1,51}$ = 12.14, P = 0.001) and site (RVDB: $F_{3,51}$ = 2.29, P = 0.001; Lazypipe: $F_{3,51}$ = 1.28, P = 0.02) explained variation between mosquito viromes. The virome communities did not demonstrate temporal differences, i.e., year (RVDB: $F_{1,51}$ = 0.09, P = 0.36; Lazypipe: $F_{1,51}$ = 0.17, P = 0.50) or season (RVDB: $F_{1,51}$ = 0.20, P = 0.81; Lazypipe: $F_{1,51}$ = 0.10, P = 0.84).

Discussion

As the geographic distribution of mosquitoes and their associated viral pathogens continues to shift, factors influencing community structure of the mosquito viromes, with respect to emergence of viral infectious diseases, need to be elucidated (27). While several recent studies described viromes of mosquito species in various regions globally (11, 49–53), few have analyzed viromes of individual mosquitoes, with respect to mosquito-specific viromes and their spatiotemporal relationships and community structure (10, 54). Next-generation RNA sequencing was employed in the study reported here, allowing detection of *ca.* 20 viral species associated with *A. albopictus* and *A. vexans* mosquitoes collected across different seasons, years, and geographical locations. Consistent with previously reported observations (11, 51, 52), viral community structure varied significantly by mosquito host species but not by year, season, or geographic location. The data indicate a stable core virome for *A. albopictus* that extends over a larger extent than previously understood – highlighting the need for information on how insect-specific viruses impact transmission of zoonotic pathogens.

Climate change and urbanization are impacting mosquito vector populations and their associated viral pathogens at an intensifying pace, underscoring the importance of knowing the baseline diversity of viruses carried by mosquito vectors to facilitate future studies of virus range shifts. Climatic conditions are proving more

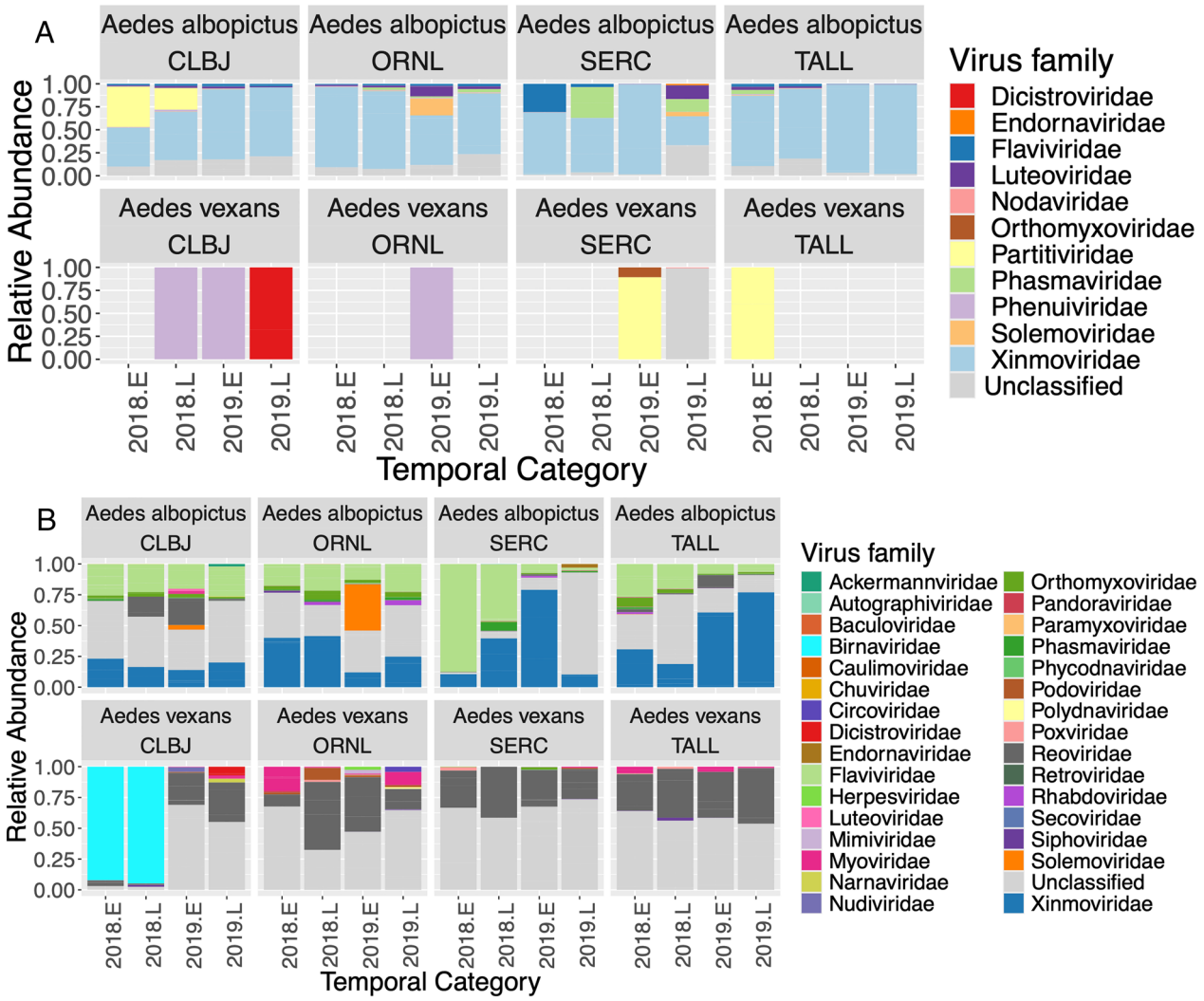

Fig. 2. Relative abundance of reads for virus families within each sampling category for (*A*) the RVDB dataset and (*B*) the Lazypipe dataset. Temporal Category indicates year followed by ".E" for early season or ".L" for late season samples. The average depth of sequencing for the CLBJ, ORNL, SCBI, SERC, and TALL samples were approximately 115 million, 107 million, 126 million, 124 million, and 110 million reads, respectively.

favorable for transmission of viruses pathogenic to humans, including West Nile virus (55), with the vectors expanding their ranges globally (56). Kraemer et al. (6) estimated that vectors, namely *Aedes aegypti* and *A. albopictus,* will have invaded a total area of 20 million km^2 by 2050, placing nearly 50% of the global population at risk of infection by the arboviruses they transmit, with even larger increases possible by 2080. Changes in both climate and environmental temperatures are also likely to mediate virus–vector interactions, influencing mosquito gene expression and the diversity of their host microorganisms (57). Future analyses using the suite of colocated weather, carbon flux, and ecosystem productivity data at NEON sites could elucidate mechanisms influencing patterns of virus distribution in the field.

Meta-omics (DNA and RNA) provide a powerful method for surveillance of microorganisms and tracking disease risk because they are culture-independent in determining viral community composition (58). Given their high rates of mutation, RNA viruses are predisposed to emergence (59). By incorporating mosquito virome ecology in viral surveillance, control measures can be more effective in meeting the challenge of vector-borne disease dynamics (27). A strong effect of mosquito species on the viral microbiome and lack of spatiotemporal influence on mosquito virome composition are consistent with the hypothesis that environmental conditions pose less of a barrier to viral introduction than the virus–vector interface. The implication is, therefore, that early detection of a novel virus employing RNAseq methods will contribute to control and subsequent development of qPCR assay for a more extensive surveillance.

The taxonomy of mosquitoes has been used to differentiate mosquito virus communities (49–52, 60–62) and several such studies have shown a stable, species-specific "core virome" (10, 51, 52, 58). In this study, a core virome of four to eight species was identified in *A. albopictus* sampled across a distance of *ca.* 2,000 km (Fig. 4). A species-specific mosquito virome should not be surprising, given that viruses recognize and enter host cells that differ across species, creating an effective host species barrier to viral infection (3, 49, 51, 52). Vector specificity may arise also from species-specific differences in vector immunity or viral genetics (63). An additional potential source of species-level variation in the mosquito virome could derive from species-specific differences in their larval habitat, which can impact exposure of the two species to different viruses (62).

Several viruses detected in *A. albopictus* have been reported in *A. albopictus* across the globe. Three were detected in all *A. albopictus* individuals analyzed in this study (Aedes flavivirus, Guato virus, and Wenzhou sobemo-like virus 4) and are listed in the top twenty viruses of *Aedes* mosquitoes compiled by Moonen et al. (21). Kaiowa virus, another *Aedes* virus (21), was detected in the *A. albopictus* of this study. *A. albopictus* anphevirus, detected in

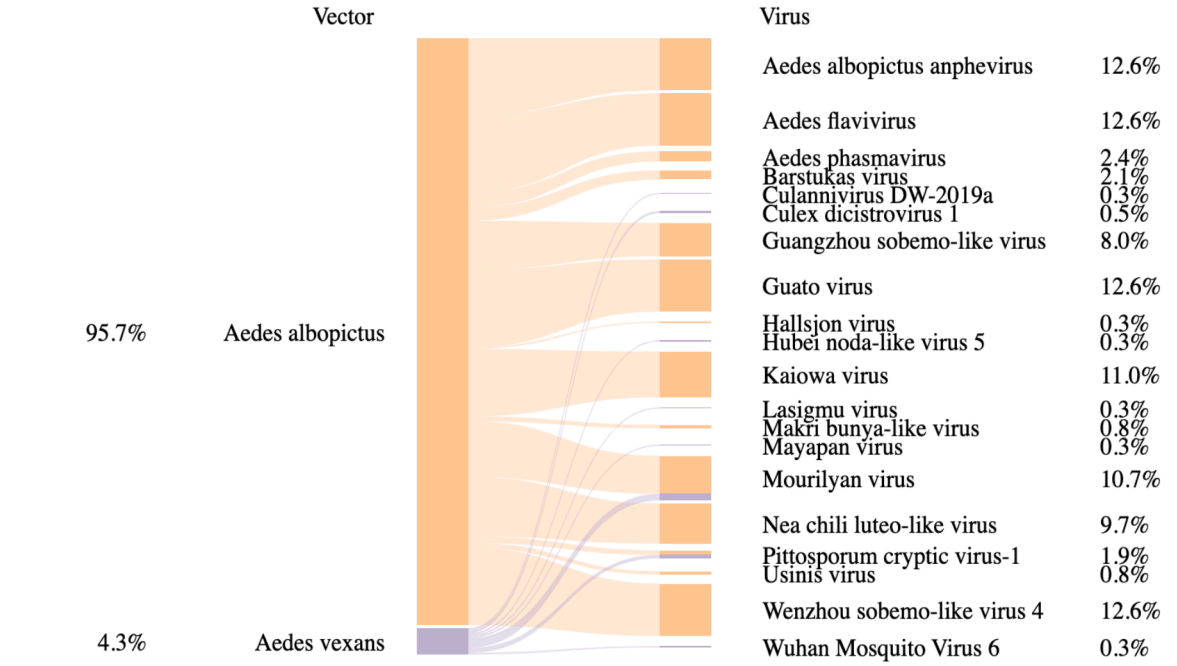

Fig. 3. Sankey diagram depicting viruses detected within each vector as percent of total vector–virus pairs (n = 373) present using the RVDB dataset.

all *A. albopictus*, also appears to be ubiquitous, having been listed in publicly available datasets representing wild-caught collections from China, Italy, Thailand, and laboratory colonies in the United States (64). Given that *A. albopictus* anphevirus can coinfect mosquitoes with Chikungunya virus and that yet another Aedes anphevirus has been reported to reduce dengue virus replication in vitro (61), further study is merited. Interestingly, the less common Usinis virus and Barstukas virus were detected in *A. albopictus* collected in China (52, 61).

Greater diversity and abundance of viruses were found in *A. albopictus* compared to *A. vexans.* Higher diversity of viruses detected in *A. albopictus* suggests possible greater permissiveness of the species to viruses (10, 28), consistent with being a notorious vector of arboviral pathogens. Interestingly, a study done in China found no difference in the viral diversity of *A. vexans* and *A. albopictus*. However, the same study reported higher viral diversity in *A. albopictus* in the United States than China (52). Clearly, the role species plays in mosquito virome diversity merits study, particularly whether it derives from differences in exposure (62), perhaps in the larval habitat, or host-specific barrier to infection (3).

Spatiotemporal factors and mosquito virome species composition over larger geographic scales have been less commonly studied, with conflicting observations and conclusions (10). In contrast to findings of this study, distinctive seasonal virome patterns for *A. albopictus* (49, 65) and an impact of location on viral

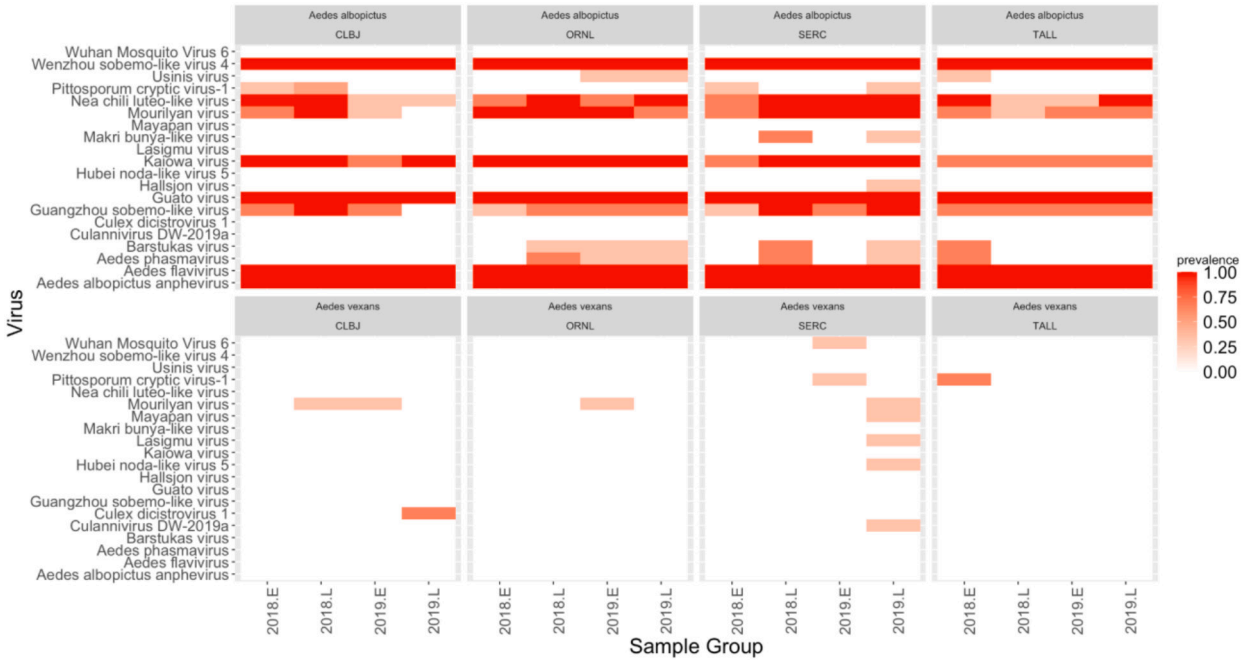

Fig. 4. Heatmap showing proportion of mosquitoes and virus species in each sample group using the RVDB dataset. Sample Group indicates the year followed by ".E" for early season or ".L" for late season samples.

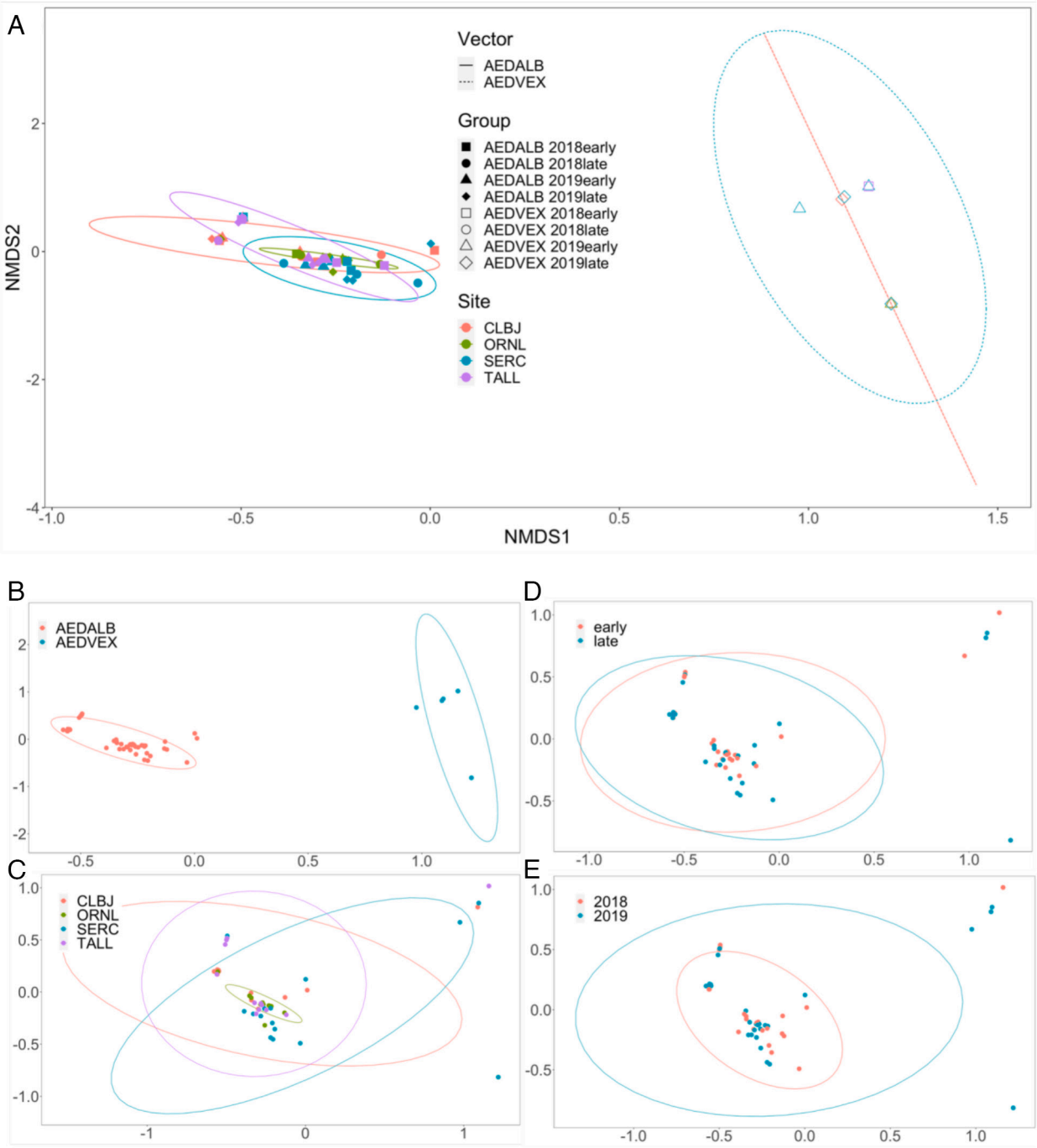

Fig. 5. NMDS plots of mosquito viromes using the RVDB dataset grouped by (*A*) spatiotemporal category and species, where species are depicted with filled or open symbols, site with color, and time with differently shaped symbols. Additional diagrams show the same data by (*B*) species, (*C*) site, (*D*) time of season, and (*E*) year. Ellipses indicate 95% CI. The stress value is 0.06.

community structure have been reported (50, 60, 66). Environmental temperature, availability of food resources, age of mosquitoes, and mosquito population densities are seasonally variable, hence potential contributors to shifts in the mosquito virome (24, 49). Viruses present year-round suggest lack of adaptive mosquito population immunity, low fitness cost of the virus, or transovarial transmission between mosquitoes and their offspring playing possible roles (49). Other studies reported no significant variation across locations, consistent with findings of this study (51, 61, 65).

Depletion of mosquito RNA through subtractive hybridization enabled higher coverage of microbial RNA than ribosomal RNA depletion methods described elsewhere. The rRNA depletion method of Thongsripong et al. (51) removed mosquito small ribosomal subunit rRNA, increasing average percentage of virus reads in the total reads per sample from 0.095 ± 0.160% (N = 12 samples) in untreated samples to 0.438 ± 0.661% (N = 18 samples) in treated samples. Here, the method used yielded virus reads comprising 92.4 ± 12.9% of the total reads per sample (N = 95), with none of the reads aligning to any portion of either mosquito genome after subtractive hybridization. Thus, subtractive hybridization, as described, provided improved virome analysis when monitoring potential viral pathogen spread in vector populations. This subtractive hybridization can advance biosurveillance since next-generation sequencing to a depth required for viral genome

surveillance is cost-prohibitive. Higher percentage of viral RNA in the RNAseq library allowed lower sequencing depth. However, subtractive hybridization may remove RNA of viral origin, which must be considered to avoid bias. Further, the methodology employed in this study would have filtered out viral introgression into the mosquito genome; a better understanding of the extent of introgression merits future study.

Limitations of the study reported here are worth noting. While this study did not uncover novel viruses in the subset of 95 mosquitos analyzed, the Lazypipe viral discovery methodology is highly generalized across taxa. Development of a pipeline specific to mosquitoes can facilitate future viral discovery. Further study should determine whether the relatively low diversity of viruses detected in *A. vexans* reflects database limitations considering relatively high research investment in the invasive vector, *A. albopictus* (28), and the higher number of unclassified reads in the *A. vexans* library. Additionally, while the 2,000 km spatial scale of the dataset employed in this study is one of the more expansive to date, a longer time series with additional individual replicates and continental-scale coverage would provide a greater capacity to uncover spatiotemporal trends in virome community structure, particularly with respect to the more rare viruses. Large-scale observatories like NEON are a valuable resource and well poised to enable studies as reported here because of the standardized framework employed in the collection and handling of mosquito specimens enabling virome comparison across multiple scales.

In summary, RNA sequencing provides a powerful tool to understand how and when viruses use new hosts, and permissiveness of mosquitoes for different viruses (10), as well as the influence of insect-specific viruses on mosquito physiology and arboviral transmission (21, 26, 67). Results of sequencing the metatranscriptome of individual mosquitoes over large spatial scales provide evidence of the spatial distribution of core viromes and the ecological scale within which mosquito virus dynamics operate. Continued surveillance of viruses from individual mosquitoes or small pools of mosquitoes using shotgun metagenomics and metatranscriptomics will allow an extensive identification of novel viruses or arbovirus precursor (22, 28). Studies conducted over continental spatial scales and multiannual time scales will improve understanding of shifting mosquito virus dynamics during climate change and urbanization. Geographic comparisons exploiting data available from NEON provide a valuable step forward in understanding both the biology of these viruses and their ecology.

Data, Materials, and Software Availability. Sequencing data generated for all samples included in this study have been deposited in NCBI Sequence Read Archive Database under BioProject ID PRJNA1066886 (68). Sample attributes and accession numbers can be found in the supporting information.

ACKNOWLEDGMENTS. The National Ecological Observatory Network (NEON) is a program sponsored by the NSF and operated under cooperative agreement by Battelle. The NEON Biorepository at Arizona State University provided samples and data collected as part of the NEON Program. We also thank the Battelle Independent Research & Development (IRAD) Program for funding. NSF (Award Nos. OCE1839171 and CCF1918749) and the NASA (Award Nos. 80NSSC20K0814 and 80NSSC22K1044) are also gratefully acknowledged. We would also like to express appreciation for our manuscript reviewers: Dr. Stefan Green as well as two anonymous reviewers for providing extremely helpful feedback.

Author affiliations: [a]Battelle, National Ecological Observatory Network, Boulder, CO 80301; [b]Battelle, Health, Drug Development, and Precision Diagnostics, Columbus, OH 43201; [c]EZBiome Inc, Gaithersburg, MD 20878; [d]Department of Cellular Biology and Molecular Genetics (CBMG), University of Maryland Institute for Advanced Computer Studies (UMIACS), College Park, MD 20742; and [e]Battelle, National Security—Chemical, Biological, Radiological, Nuclear and Explosives, Columbus, OH 43201

1. S. C. Weaver, Urbanization and geographic expansion of zoonotic arboviral diseases: Mechanisms and potential strategies for prevention. *Trends Microbiol.* **21**, 360–363 (2013).
2. S. Leta *et al.*, Global risk mapping for major diseases transmitted by *Aedes aegypti* and *Aedes albopictus*. *Int. J. Infectious Dis.* **67**, 25–35 (2018).
3. C. Rückert, G. D. Ebel, How do virus–mosquito interactions lead to viral emergence? *Trends Parasitol.* **34**, 310–321 (2018).
4. H. Ketkar, D. Herman, P. Wang, Genetic determinants of the re-emergence of arboviral diseases. *Viruses* **11**, 150 (2019).
5. S. J. Ryan, C. J. Carlson, E. A. Mordecai, L. R. Johnson, Global expansion and redistribution of *Aedes*-borne virus transmission risk with climate change. *PLoS Negl. Trop Dis.* **13**, e0007213 (2019).
6. M. U. G. Kraemer *et al.*, Past and future spread of the arbovirus vectors *Aedes aegypti* and *Aedes albopictus*. *Nat. Microbiol.* **4**, 854–863 (2019).
7. J. Thannesberger *et al.*, Viral metagenomics reveals the presence of novel Zika virus variants in *Aedes* mosquitoes from Barbados. *Parasites Vectors* **14**, 343 (2021).
8. W. Gu, S. Miller, C. Y. Chiu, Clinical metagenomic next-generation sequencing for pathogen detection. *Annu. Rev. Pathol.: Mech. Dis.* **14**, 319–338 (2019).
9. P. J. Simner, S. Miller, K. C. Carroll, Understanding the promises and hurdles of metagenomic next-generation sequencing as a diagnostic tool for infectious diseases. *Clin. Infectious Dis.* **66**, 778–788 (2018).
10. J. P. De Almeida, E. R. Aguiar, J. N. Armache, R. P. Olmo, J. T. Marques, The virome of vector mosquitoes. *Curr. Opin. Virol.* **49**, 7–12 (2021).
11. K. Konstantinidis *et al.*, Defining virus-carrier networks that shape the composition of the mosquito core virome of a local ecosystem. *Virus Evol.* **8**, veac036 (2022).
12. H. Bedir, B. Demirci, Z. Vatansever, Host-feeding patterns of mosquito species in Aras Valley, Turkey. *JERS* **24**, 303–320 (2022).
13. K. Fikrig *et al.*, *Aedes albopictus* host odor preference does not drive observed variation in feeding patterns across field populations. *Sci. Rep.* **13**, 130 (2023).
14. T. Pereira-dos-Santos, D. Roiz, R. Lourenço-de-Oliveira, C. Paupy, A systematic review: Is *Aedes albopictus* an efficient bridge vector for zoonotic arboviruses? *Pathogens* **9**, 266 (2020).
15. G. Giunti, N. Becker, G. Benelli, Invasive mosquito vectors in Europe: From bioecology to surveillance and management. *Acta Tropica* **239**, 106832 (2023).
16. T. G. Andreadis, J. F. Anderson, C. R. Vossbrinck, A. J. Main, Epidemiology of West Nile virus in Connecticut: A five-year analysis of mosquito data 1999–2003. *Vector-Borne Zoonotic Dis.* **4**, 360–378 (2004).
17. A. Gendernalik *et al.*, American *Aedes vexans* mosquitoes are competent vectors of Zika virus. *Am. J. Tropical Med. Hygiene* **96**, 1338–1340 (2017).
18. A. Drouin, V. Chevalier, B. Durand, T. Balenghien, Vector competence of mediterranean mosquitoes for Rift Valley fever virus: A meta-analysis. *Pathogens* **11**, 503 (2022).
19. N. Ledesma, L. Harrington, Mosquito vectors of dog heartworm in the United States: Vector status and factors influencing transmission efficiency. *Top. Companion Animal Med.* **26**, 178–185 (2011).
20. A. Outammassine, S. Zouhair, S. Loqman, Global potential distribution of three underappreciated arboviruses vectors (Aedes japonicus, Aedes vexans and Aedes vittatus) under current and future climate conditions. *Transbound. Emerg. Dis.* **69**, e1160–e1171 (2022).
21. J. P. Moonen, M. Schinkel, T. Van Der Most, P. Miesen, R. P. Van Rij, Composition and global distribution of the mosquito virome – A comprehensive database of insect-specific viruses. *One Health* **16**, 100490 (2023).
22. B. Bolling, S. Weaver, R. Tesh, N. Vasilakis, Insect-specific virus discovery: Significance for the arbovirus community. *Viruses* **7**, 4911–4928 (2015).
23. L. De Coninck *et al.*, Lack of abundant core virome in *Culex* mosquitoes from a temperate climate region despite a mosquito species-specific virome. *mSystems* **9**, e00012-24 (2024).
24. M. Guégan *et al.*, The mosquito holobiont: Fresh insight into mosquito-microbiota interactions. *Microbiome* **6**, 49 (2018).
25. P. Burivong, S.-N. Pattanakitsakul, S. Thongrungkiat, P. Malasit, T. W. Flegel, Markedly reduced severity of Dengue virus infection in mosquito cell cultures persistently infected with Aedes albopictus densovirus (AalDNV). *Virology* **329**, 261–269 (2004).
26. Leggewie Agboli, Altinli, Schnettler, mosquito-specific viruses–Transmission and interaction. *Viruses* **11**, 873 (2019).
27. E. I. Patterson, J. Villinger, J. N. Muthoni, L. Dobel-Ober, G. L. Hughes, Exploiting insect-specific viruses as a novel strategy to control vector-borne disease. *Curr. Opin. Insect Sci.* **39**, 50–56 (2020).
28. M. Gómez, D. Martinez, M. Muñoz, J. D. Ramírez, *Aedes aegypti* and *Ae. albopictus* microbiome/virome: New strategies for controlling arboviral transmission? *Parasites Vectors* **15**, 287 (2022).
29. K. LeVan, *TOS Protocol and Procedure: Mosquito Sampling. NEON.DOC.014049vM* (National Ecological Observatory Network, 2019).
30. NEON Biorepository Data Portal, NEON Biorepository Mosquito Collection (Bulk Identified). Occurrence dataset https://doi.org/10.15468/m967up accessed via the NEON Biorepository Data Portal, https://biorepo.neonscience.org/ (2023).
31. P. H. Culviner, C. K. Guegler, M. T. Laub, A simple, cost-effective, and robust method for rRNA depletion in RNA-sequencing studies. *mBio* **11**, e00010–20 (2020).
32. K. D. Brumfield *et al.*, Gut microbiome insights from 16S rRNA analysis of 17-year periodical cicadas (Hemiptera: Magicicada spp.) Broods II, VI, and X. *Sci. Rep.* **12**, 16967 (2022).
33. D. E. Wood, J. Lu, B. Langmead, Improved metagenomic analysis with Kraken 2. *Genome Biol.* **20**, 257 (2019).
34. M. Chalita *et al.*, Improved metagenomic taxonomic profiling using a curated core gene-based bacterial database reveals unrecognized species in the genus *Streptococcus*. *Pathogens* **9**, 204 (2020).
35. S.-H. Yoon *et al.*, Introducing EzBioCloud: A taxonomically united database of 16S rRNA gene sequences and whole-genome assemblies. *Int. J. Syst. Evol. Microbiol.* **67**, 1613–1617 (2017).
36. B. Langmead, S. L. Salzberg, Fast gapped-read alignment with Bowtie 2. *Nat. Methods* **9**, 357–359 (2012).

37. H. Li *et al.*, The sequence alignment/map format and SAMtools. *Bioinformatics* **25**, 2078–2079 (2009).
38. A. R. Quinlan, I. M. Hall, BEDTools: A flexible suite of utilities for comparing genomic features. *Bioinformatics* **26**, 841–842 (2010).
39. I. Plyusnin *et al.*, Novel NGS pipeline for virus discovery from a wide spectrum of hosts and sample types. *Virus Evol.* **6**, veaa091 (2020).
40. S. Chen, Y. Zhou, Y. Chen, J. Gu, fastp: An ultra-fast all-in-one FASTQ preprocessor. *Bioinformatics* **34**, i884–i890 (2018).
41. D. Li, C.-M. Liu, R. Luo, K. Sadakane, T.-W. Lam, MEGAHIT: An ultra-fast single-node solution for large and complex metagenomics assembly via succinct *de Bruijn* graph. *Bioinformatics* **31**, 1674–1676 (2015).
42. H. Li, Aligning sequence reads, clone sequences and assembly contigs with BWA-MEM. bioXriv [Preprint] (2013). http://arxiv.org/abs/1303.3997 [Accessed 29 September 2023].
43. D. Kim, L. Song, F. P. Breitwieser, S. L. Salzberg, Centrifuge: Rapid and sensitive classification of metagenomic sequences. *Genome Res.* **26**, 1721–1729 (2016).
44. S. F. Altschul, W. Gish, W. Miller, E. W. Myers, D. J. Lipman, Basic local alignment search tool. *J. Mol. Biol.* **215**, 403–410 (1990).
45. N. Goodacre, A. Aljanahi, S. Nandakumar, M. Mikailov, A. S. Khan, A Reference viral database (RVDB) to enhance bioinformatics analysis of high-throughput sequencing for novel virus detection. *mSphere* **3**, e00069-18 (2018)
46. NEON (National Ecological Observatory Network). Mosquito pathogen status (DP1.10041.001), RELEASE-2023. https://doi.org/10.48443/k4gc-r927. Dataset accessed from https://data.neonscience.org/data-products/DP1.10041.001/RELEASE-2023 on December 11, 2023.
47. J. Oksanen *et al.*, vegan: Community Ecology Package_R package version 2.6-4. (2022). https://github.com/vegandevs/vegan. Accessed 24 June 2022.
48. R Core Team, R A language and environment for statistical computing. (2022), Deposited 2022.
49. Y. Feng *et al.*, A time-series meta-transcriptomic analysis reveals the seasonal, host, and gender structure of mosquito viromes. *Virus Evol.* **8**, veac006 (2022).
50. S. M. Abel *et al.*, Small RNA sequencing of field *Culex* mosquitoes identifies patterns of viral infection and the mosquito immune response. *Sci. Rep.* **13**, 10598 (2023).
51. P. Thongsripong *et al.*, Metagenomic shotgun sequencing reveals host species as an important driver of virome composition in mosquitoes. *Sci. Rep.* **11**, 8448 (2021).
52. Q. Liu *et al.*, Association of virome dynamics with mosquito species and environmental factors. *Microbiome* **11**, 101 (2023).
53. Y. Xu, J. Xu, T. Liu, P. Liu, X.-G. Chen, Metagenomic analysis reveals the virome profiles of *Aedes albopictus* in Guangzhou, China. *Front. Cell. Infect. Microbiol.* **13**, 1133120 (2023).
54. J. Batson *et al.*, Single mosquito metatranscriptomics identifies vectors, emerging pathogens and reservoirs in one assay. *eLife* **10**, e68353 (2021).
55. S. H. Paull *et al.*, Drought and immunity determine the intensity of West Nile virus epidemics and climate change impacts. *Proc. R. Soc. B.* **284**, 20162078 (2017).
56. R. N. Cuthbert *et al.*, Invasive hematophagous arthropods and associated diseases in a changing world. *Parasites Vectors* **16**, 291 (2023).
57. R. Bellone *et al.*, Climate change and vector-borne diseases: A multi-omics approach of temperature-induced changes in the mosquito. *J. Travel Med.* **30**, taad062 (2023).
58. C. Shi *et al.*, Stability of the virome in lab- and field-collected *Aedes albopictus* mosquitoes across different developmental stages and possible core viruses in the publicly available virome data of *Aedes* mosquitoes. *mSystems* **5**, e00640-20 (2020).
59. J. Kubacki *et al.*, Viral metagenomic analysis of *Aedes albopictus* mosquitos from southern Switzerland. *Viruses* **12**, 929 (2020).
60. Shi Pettersson, Eden, Holmes, Hesson, Meta-transcriptomic comparison of the RNA viromes of the mosquito vectors *Culex pipiens* and *Culex torrentium* in Northern Europe. *Viruses* **11**, 1033 (2019).
61. C. Li *et al.*, Metatranscriptomic sequencing reveals host species as an important factor shaping the mosquito virome. *Microbiol. Spectr.* **11**, e04655-22 (2023).
62. C. Morel *et al.*, Host influence on the eukaryotic virome of sympatric mosquitoes and abundance of diverse viruses with a broad host range. *PLoS One* **19**, e0300915 (2024).
63. S. Cottis, A. A. Blisnick, A.-B. Failloux, K. D. Vernick, Determinants of Chikungunya and O'nyong-Nyong virus specificity for infection of *Aedes* and *Anopheles* mosquito vectors. *Viruses* **15**, 589 (2023).
64. M. Manni, E. M. Zdobnov, A novel anphevirus in *Aedes albopictus* mosquitoes Is distributed worldwide and interacts with the host RNA interference pathway. *Viruses* **12**, 1264 (2020).
65. W. He *et al.*, Virome in adult *Aedes albopictus* captured during different seasons in Guangzhou City, China. *Parasites Vectors* **14**, 415 (2021).
66. E. Atoni *et al.*, Metagenomic virome analysis of *Culex* mosquitoes from Kenya and China. *Viruses* **10**, 30 (2018).
67. S. Nouri, E. E. Matsumura, Y.-W. Kuo, B. W. Falk, Insect-specific viruses: From discovery to potential translational applications. *Curr. Opin. Virol.* **33**, 33–41 (2018).
68. S. H. Paull *et al.*, Metatranscriptomic analysis of *Aedes albopictus* and *Aedes vexans* mosquito RNA viruses collected in the Southeastern United States by the National Ecological Observatory Network (NEON). NCBI BioProject. https://www.ncbi.nlm.nih.gov/bioproject/?term=PRJNA1066886. Accessed 24 April 2025.